

Supplemental Information

Nanoluciferase complementation-based bioreporter reveals the importance of N-linked glycosylation of SARS-CoV-2 S for viral entry

Taha Azad, Ragunath Singaravelu, Zaid Taha, Taylor R. Jamieson, Stephen Boulton, Mathieu J.F. Crupi, Nikolas T. Martin, Emily E.F. Brown, Joanna Poutou, Mina Ghahremani, Adrian Pelin, Kazem Nouri, Reza Rezaei, Christopher Boyd Marshall, Masahiro Enomoto, Rozanne Arulanandam, Nouf Alluqmani, Reuben Samson, Anne-Claude Gingras, D. William Cameron, Peter A. Greer, Carolina S. Ilkow, Jean-Simon Diallo, and John C. Bell

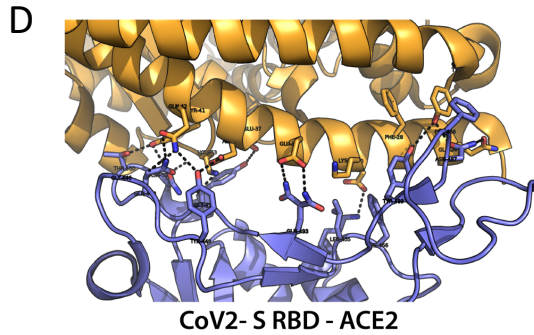
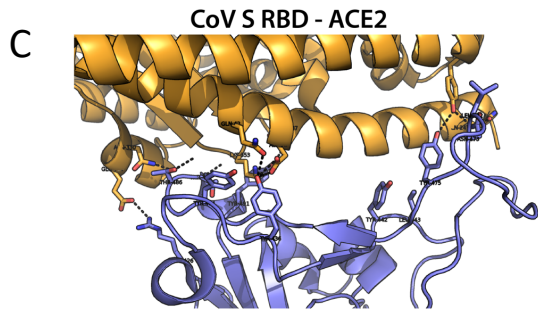
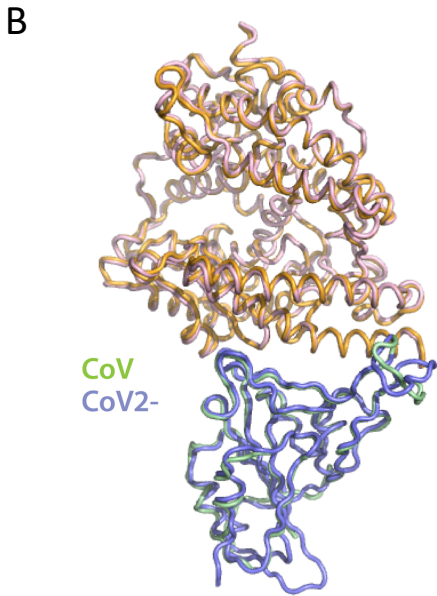
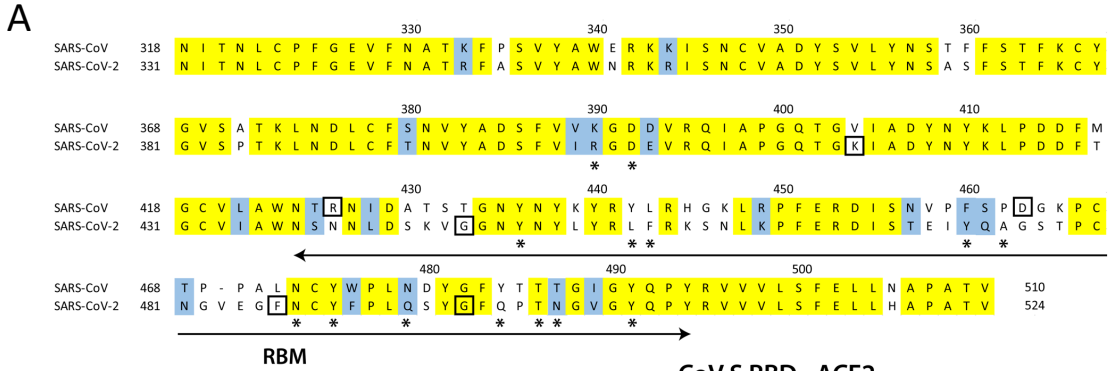


Figure S1. Structural comparison of SARS CoV and CoV-2 spike protein RBDs. (A) Sequence alignment of SARS CoV and CoV-2 spike RBDs performed with ClustalW. Yellow indicates complete identity, while blue depicts residues with similar side chain properties. The receptor binding motif (RBM) is highlighted beneath. Residues participating in the interaction with ACE2 are indicated with an asterisk if at a common site in both SARS CoV and CoV-2 or a box if unique to one RBD or another. Numbering on top of residues is based on the SARS-CoV Spike protein. (B) Alignment of tertiary structures of SARS CoV (green; PDB Id: 2AJF) and CoV-2 (blue; PDB Id: 6M0J) RBDs in complex with ACE2 (pink and orange, respectively) (Lan et al. 2020; Li et al. 2005a). Interaction sites of SARS CoV (C) and CoV-2 (D) RBDs (blue) with ACE2 (orange). Black dashed lines depict polar contacts.

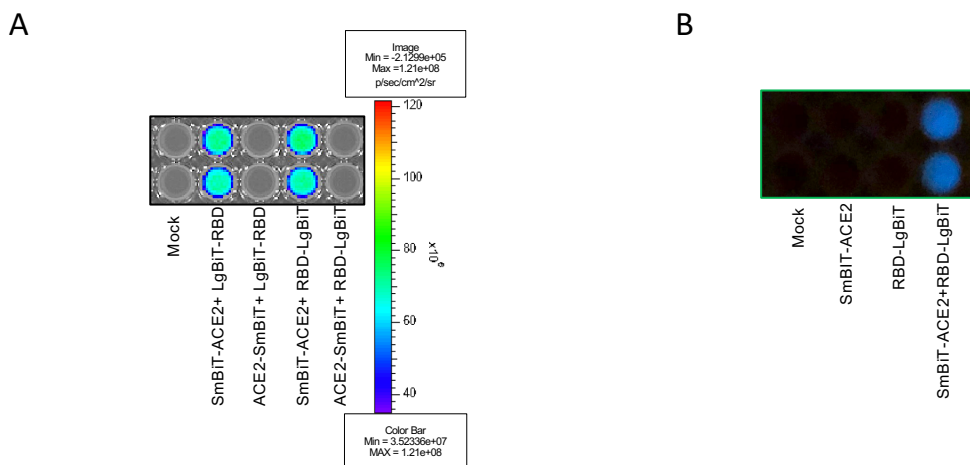


Figure S2. SARS-CoV-2 NanoBiT is compatible with alternate imaging systems. (A) 293T cells were co-transfected with constructs expressing the indicated constructs (left panel). 48 hours post-transfection, cells were lysed and FMZ was added to each well. Luminescence was visualized using the IVIS CCD camera. (B) Optimized ACE2-RBD bioreporter produces robust luminescent signal observable to naked eye. 293T cells were co-transfected with SmBiT-ACE2 and RBD-LgBiT. 50 μ g of cell lysate was incubated with FMZ (1:50 ratio) at room temperature and imaged using a standard 12MP digital phone camera.

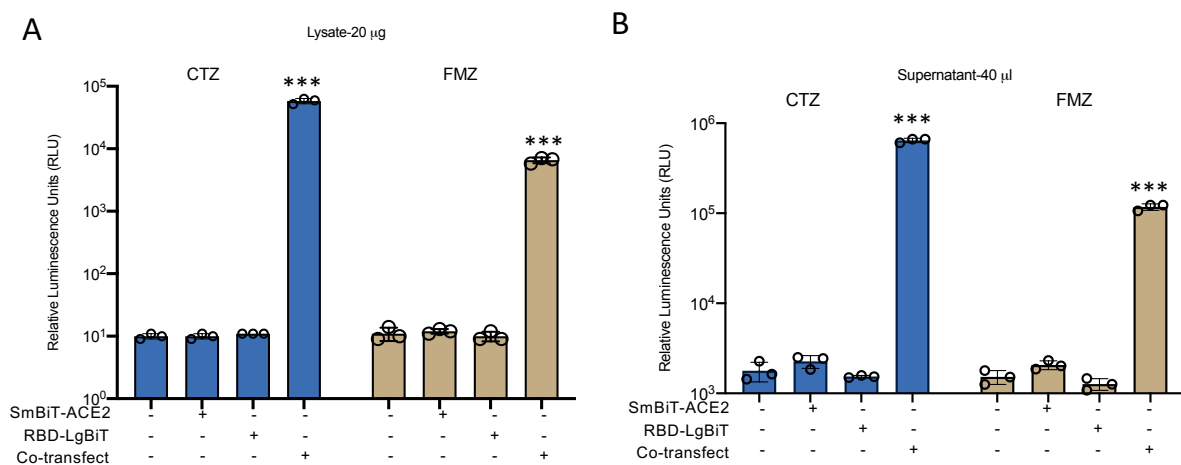


Figure S3. Comparison of substrates for Nanoluc-based reporter assay. (A) 293T cells were transfected as indicated (SmBiT-ACE2, RBD-LgBiT or co-transfected). 20 μ g of lysates were read by the addition of equal volume of substrate: coelenterazine (CTZ, blue) or furimazine (FMZ, brown). (n=3 technical replicates, mean \pm SD; one-way ANOVA, *** $p < 0.005$ relative to RBD-LgBiT alone, Dunnett's correction for multiple comparisons). Assays performed with CTZ and FMZ were analyzed independently. (B) 40 μ l of supernatant from transfected 293T cells in panel A were harvested and read similarly (n=3 technical replicates, mean \pm SD; one-way ANOVA, *** $p < 0.005$, ** $p < 0.01$ relative to RBD-LgBiT alone, Dunnett's correction for multiple comparisons). Assays performed with CTZ and FMZ were analyzed independently.

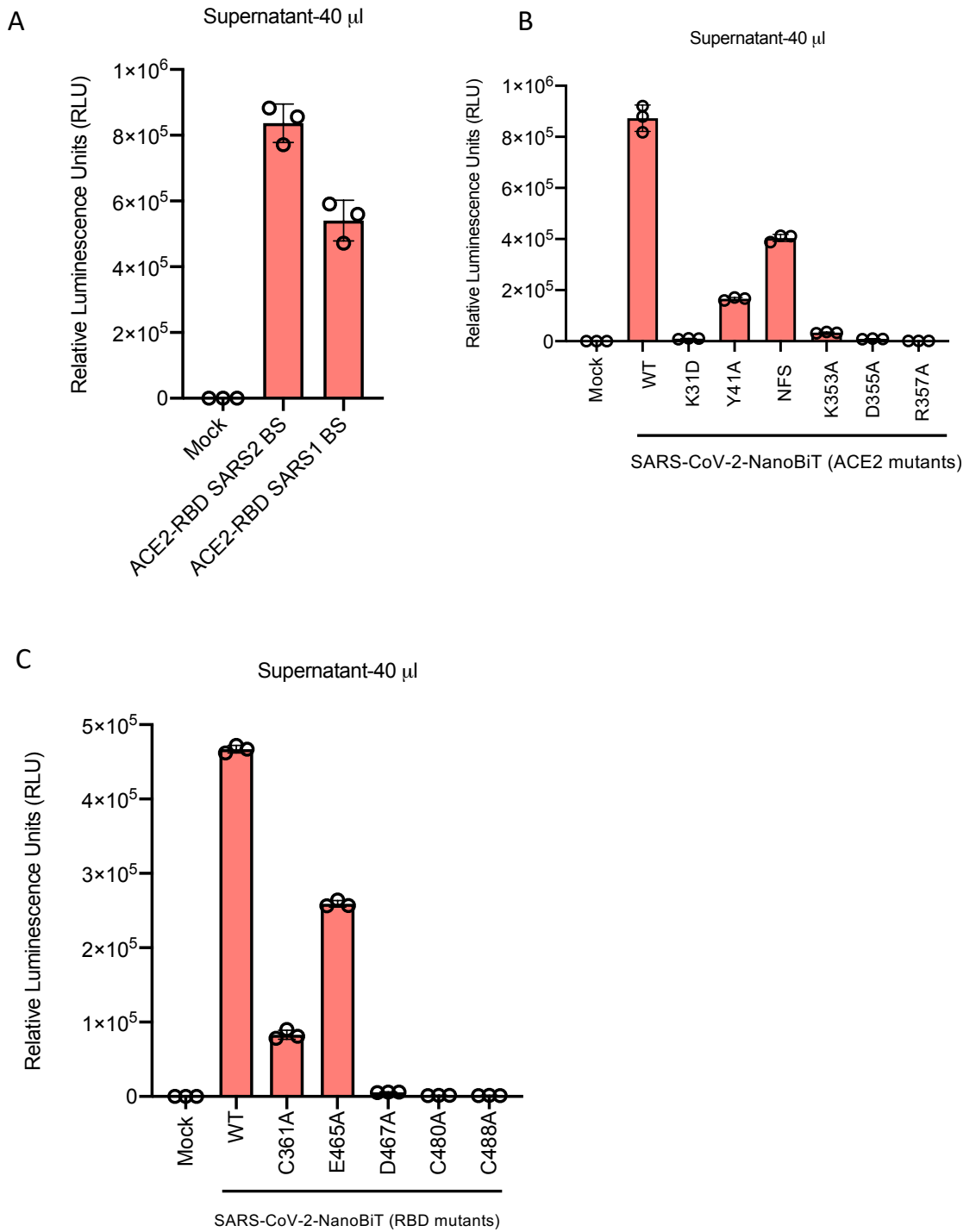


Figure S4. Development of SARS-CoV bioreporter (A) Bioreporter assay was performed on supernatant of 293T cells co-transfected with SmBiT-ACE2 and either SARS-CoV or SARS-CoV-2 RBD-LgBiT constructs, respectively. (B-C) Bioreporter assay were performed on cells co-transfected with SmBiT-ACE2 (B) or RBD-LgBiT (C) mutant constructs.

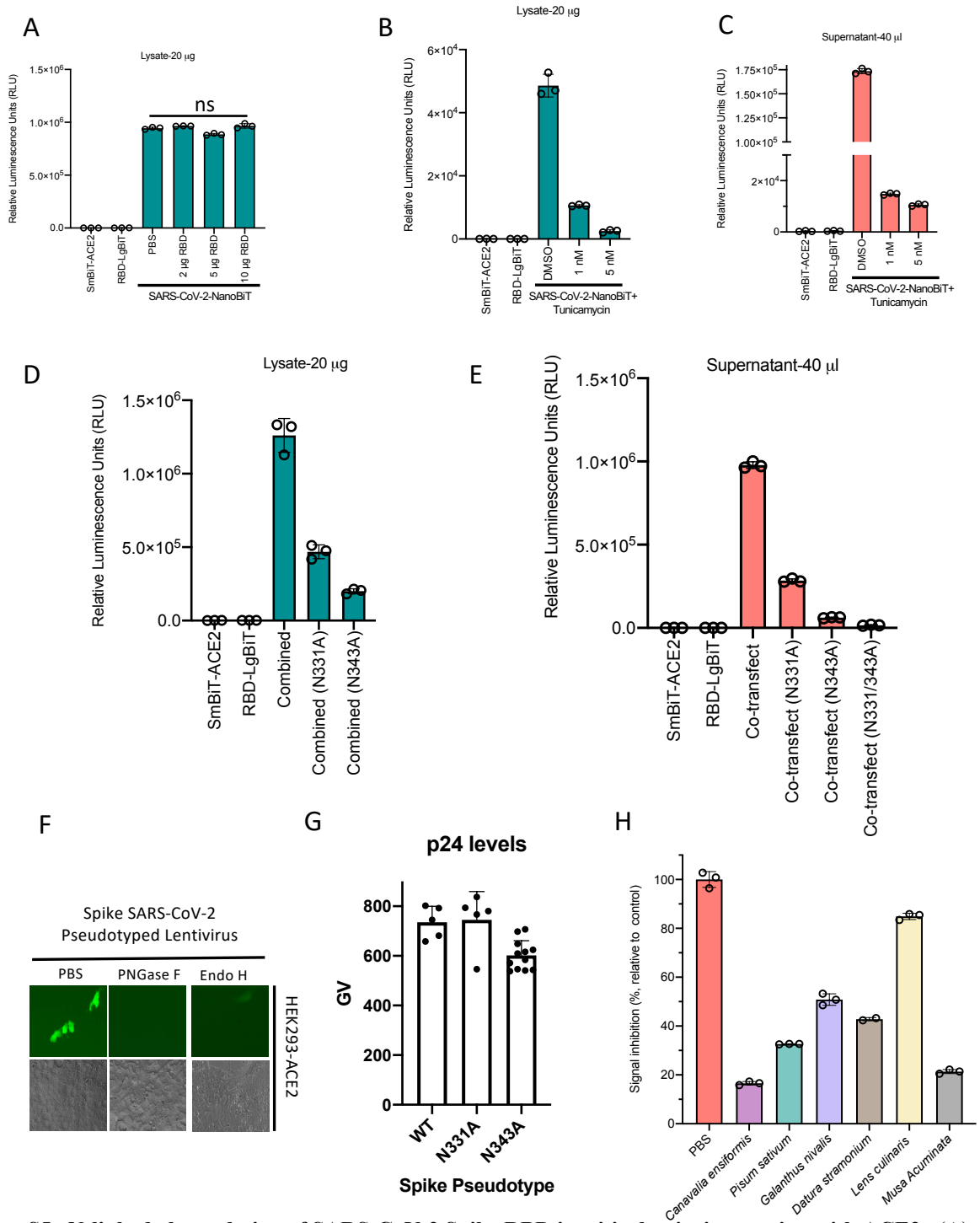
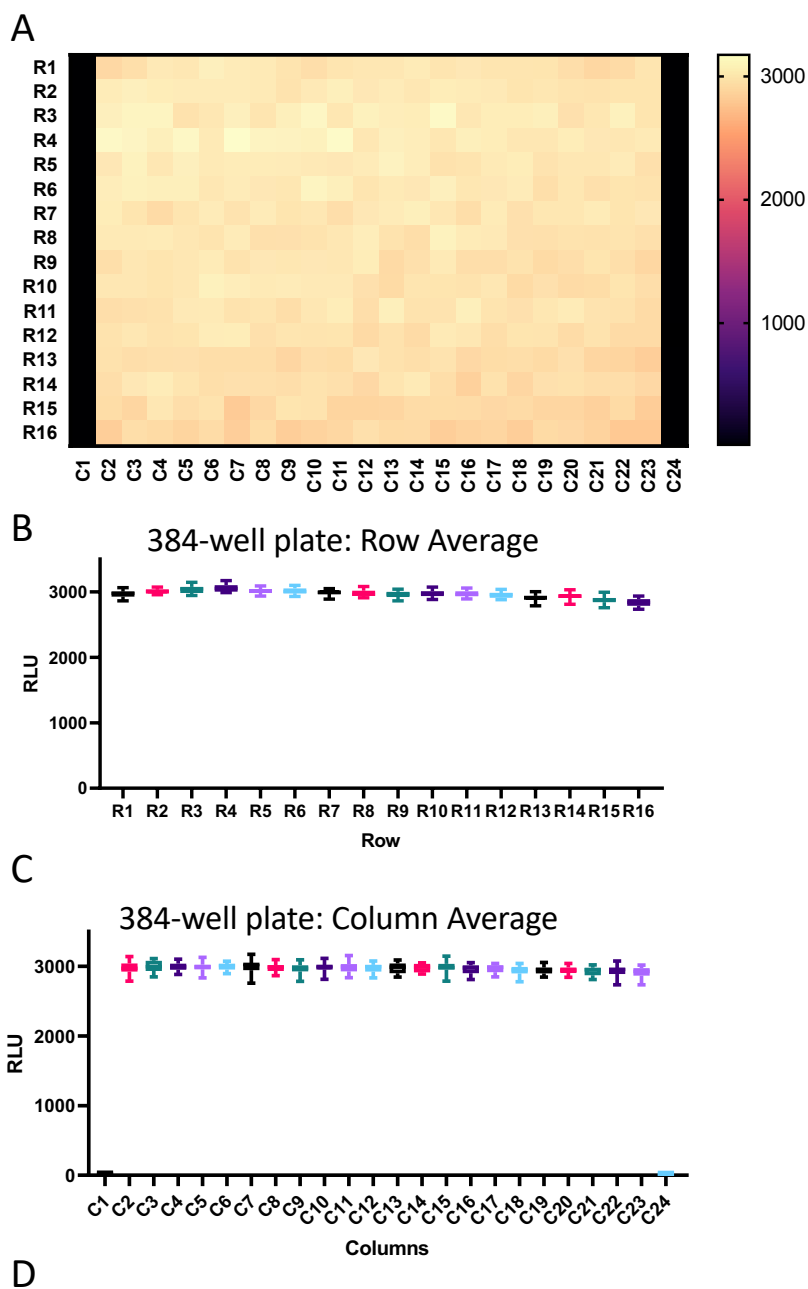


Figure S5. N-linked glycosylation of SARS-CoV-2 Spike RBD is critical to its interaction with ACE2. (A) Recombinant RBD purified from *E. coli* was incubated for 15 minutes with cell lysate containing SmBiT-ACE2 at room temperature. Equal amounts of lysates containing RBD-LgBiT were then added and incubated for 5 minutes. Luciferase assay was performed using CTZ as substrate. (n=3 biological replicates, mean \pm SD; one-way ANOVA, *** $p < 0.005$, Tukey's correction for multiple comparisons.) (B)-(C) 293T cells were transfected with RBD-LgBiT and subsequently treated with tunicamycin. (B) Lysates were combined with lysates from 293T cells transfected with SmBiT-ACE2 and the bioreporter assay was performed. (C) Analogously, supernatants were combined with supernatants from 293T cells transfected with SmBiT-ACE2 and the bioreporter assay was performed. (D) Bioreporter assay was performed on lysates from 293T cells co-transfected with the indicated RBD-glycosylation site mutant-LgBiT constructs and SmBiT-ACE2 constructs. (E) Bioreporter assay was performed on supernatants from 293T cells co-transfected with RBD-glycosylation site mutant-LgBiT constructs and SmBiT-ACE2 constructs. (F) SARS-CoV-2 S pseudotyped lentivirus encoding ZsGreen and luciferase reporters was incubated with PBS, PNGase F, or Endo H for 1 hour, and then used to infect HEK293T-ACE2 cells. 48 hours post-transduction, cells were evaluated for GFP. (G) Lentivirus levels of Spike mutant pseudotypes were titered via p24 ELISA. (H) Plant lectins were screened for ability to disrupt CoV-NanoBiT. Cell supernatants from cells transfected with RBD-LgBiT were incubated for 1 hr with different lectins from shown species. Luciferase assays were performed 5 minutes after SmBiT-ACE2 containing supernatant addition.



D

Format	384-well plate
Mean	2967.15
STDev	73.5
%CV	2.48%

Figure S6. High reproducibility and low variability associated with data generated by the SARS-CoV-2-NanoBiT bioreporter

(A) 384-well plate loaded with 20 μg of total protein from whole cell lysates isolated from HEK293T cells transfected with RBD-LgBiT, followed by addition of 20 μg total protein from whole cell lysates from HEK293T cells transfected with SmBiT-ACE2. Plates were incubated at room temperature for 20 minutes, followed by addition of CTZ substrate. Luminescence is displayed in heat map format. First and last columns of the plates were blanks. (B) The luminescence values of the rows from (A) were averaged and plotted to identify row effects, if any. (C) The luminescence values of the columns from (A) were averaged and plotted to identify any column effects. (D) Summary statistics were generated for (A). The low standard deviation and coefficient of variation of signal across the plate are suggestive of low assay variability and high reproducibility.

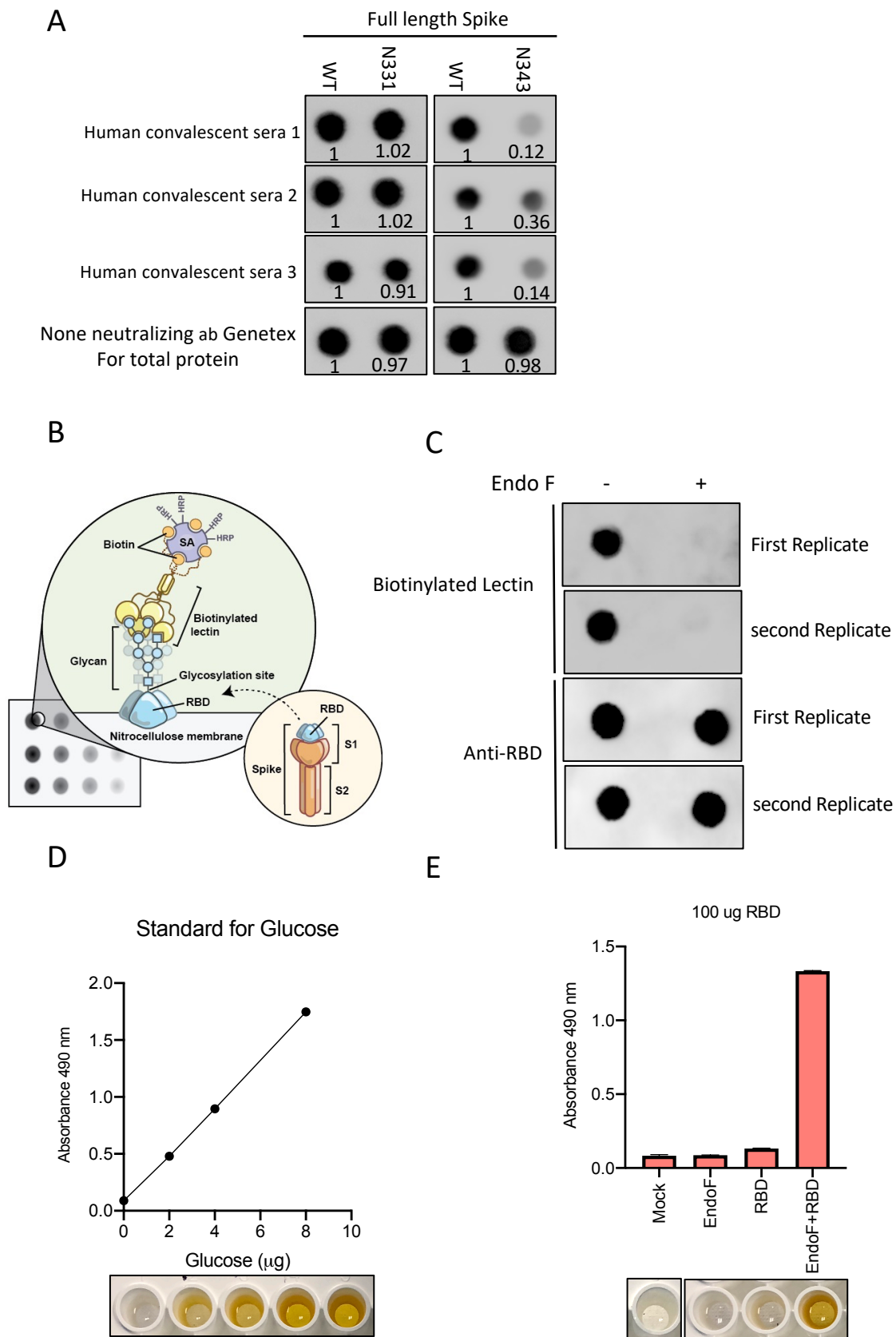


Figure S7. N-linked glycosylation is critical to antigenic conformation of RBD.

(A) Dot blot analysis comparing antibody recognition of full-length of wildtype and mutant (N331A or N343A) Spike. Lysates from HEK293T cells transfected with either wildtype or mutant Spike expression constructs were probed with human serum from convalescent COVID-19 patients ($n = 3$) or a non-neutralizing antibody from GeneTex. (B) Schematic illustrating concept of biotinylated lectin-based dot blot analysis for confirmation of Endo F-catalyzed deglycosylation of recombinant mammalian RBD. (C) Dot blot analysis comparing lectin's affinity to untreated and Endo F-treated RBD. Total RBD levels are shown as a loading control. (D) Glucose standard curve results from total carbohydrate assay kit. (E) Endo F treatment was performed on RBD and glycan release was measured using total carbohydrate assay.